Available online at www.sciencedirect.com
SCIENCE DIRECT
Polymer 46 (2005) 9810–9820
polymer
www.elsevier.com/locate/polymer

Synthesis and characterization of alternating fluorene-based copolymers containing diaryl- and non-substituted bithiophene units

Hong-Cheu Lin*, Hsiao-Hsien Sung, Chien-Min Tsai, Kuang-Chieh Li

Department of Materials Science and Engineering, National Chiao Tung University, Hsinchu, Taiwan, ROC

Received 10 June 2005; received in revised form 22 July 2005; accepted 25 July 2005
Available online 11 August 2005

Abstract

A series of soluble alternating fluorene-based copolymers containing diaryl- and non-substituted bithiophene units are synthesized by palladium-catalyzed Suzuki coupling reaction. All polymers demonstrate green colors of photoluminescence (PL) in chloroform, good thermal stability (with decomposition temperatures above 436 °C), and high glass transition temperatures (in the range of 120–144 °C). Owing to the large steric hindrance of diaryl substituents on bithiophenes in the polymers (**P2**–**P4**), the aggregation of solids is reduced as well as the solubility is improved, so the performance of their PLED devices are superior to that of the non-substituted polymer (**P1**). Compared with **P1**, the introduction of substitutents at 3,3′-position of bithiophene in **P2**–**P4** has significant effects on the photophysical properties of resulting polymers in solution and solid states. Though the PL quantum yield of **P1** is much higher than those of diaryl-substituted polymers (**P2**–**P4**), the PLED device of **P1** has the worst electroluminescence (EL) properties due to the poor solubility of **P1**. Consequently, among these polymers, the device made of **P3** as an emitter has the highest luminance of 2590 cd/m^2 at 9.5 V. For optimum device performance, a device of **P3** blended with PVK can be further enhanced to a brighter luminance of 4284 cd/m^2 at 18 V.
© 2005 Elsevier Ltd. All rights reserved.

Keywords: Alternating fluorene-based copolymers; Bithiophene; Diaryl substituents

1. Introduction

Poly(fluorene) (PF) is a well-known hole transporting blue-emitting material for polymeric light-emitting diodes (PLEDs) application [1,2]. This material displays extremely high photoluminescence (PL) efficiencies in both solution and solid states [3,4]. However, PF has some drawbacks, such as aggregation and excimer formation in the solid state [5], high energy barrier for hole injection [6–8], and unbalance charge mobilities between holes and electrons [9]. Fortunately, these unfavorable issues can be overcome by proper molecular design, i.e. fluorene monomers copolymerize with other monomers to form copolymers or introduction of electron-deficient oxadiazoles (OXD) groups into C-9 position of the fluorene units to balance charge injection and transportation as well as recombination of resulting polymers [10–12].

Polythiophenes and their derivatives have a number of interesting properties [13–15], such as relatively high conductivity and stability under ambient atmosphere along with easy preparation and tailoring of band gaps by adjusting chemical structures of the monomers [14,15]. Nevertheless, the quantum yields of these polymers are far from unity [16]. Therefore, in order to increase the quantum yields of polythiophenes, thiophene monomers can be copolymerized with monomers possessing high quantum yields, such as fluorene monomers. Besides, the π-excessive thiophene rings [17] can help lowering the oxidation potentials of the fluorene moieties, and the onset potential values of PFO are reported around 1.4 V [18].

In order to obtain highly efficient PLED devices, it is important to suppress the intermolecular interactions (aggregation between molecules), which results in the formation of excimers in the solid state and consequently lower the quantum yields of the polymers. Hence, the introduction of large substituted groups into conjugated polymers has been utilized to a great extent in controlling their physical and electronic properties [19]. In addition,

* Corresponding author. Tel.: +886 3 5712121x55305; fax: +886 3 5724727.
E-mail address: linhc@cc.nctu.edu.tw (H.-C. Lin).

0032-3861/$ - see front matter © 2005 Elsevier Ltd. All rights reserved.
doi:10.1016/j.polymer.2005.07.075

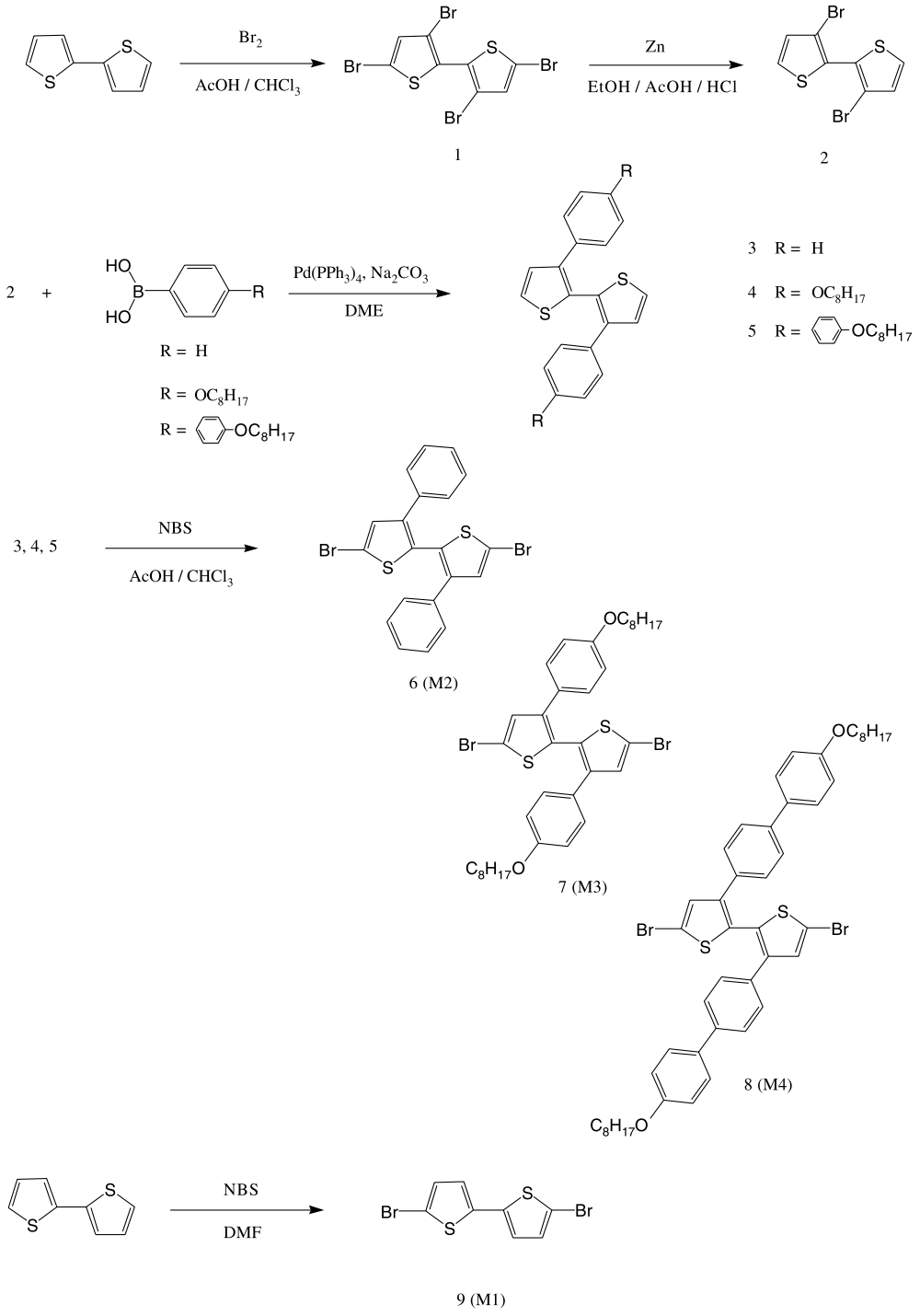

Scheme 1. Synthetic routes of monomers.

large steric hindrance of lateral substitution will reduce crystallinity in the resulting polymers and provide the polymer films with amorphous properties [19–22]. From previous studies, it is known that anti-type bithiophene units have a dihedral angle of $\theta = 147.9°$ between these two thiophene rings [23], and 3,3′-diphenyl-2,2′-bithiophene lies in an anti conformation with a dihedral angle of $\theta = 153°$ [16]. Such a conformation of these two bulky substituents at 3,3′-position of bithiophene can provide large steric hindrance to restrain interchain interaction in the solid state.

To control the emitting colors of light-emitting polymers, the most effective means is to introduce monomers with different functional groups and flexible parts as side chains to control the conjugation lengths. In addition, the regioregularity is also an important factor to control the conjugation length along the polymer backbone. To our

knowledge, very few literatures regarding copolymers containing fluorene and bithiophene units were investigated, and only related alternating copolymers of fluorenone and dialkylbithiophene have been reported [24,25]. In this work, the synthesis and characterization of four alternating fluorene-based conjugated polymers containing regioregular head-to-head coupling bithiophene with different substituents at 3,3′-position of bithiophene in the backbone are reported. The effects of substituents on the electrochemical, photophysical, and electroluminescent (EL) properties of resulting polymers are also investigated.

2. Experimental

2.1. Measurements

^{1}H NMR spectra were recorded on a Varian unity 300 MHz spectrometer using $CDCl_3$ solvent. Elemental analyses were performed on a HERAEUS CHN-OS RAPID elemental analyzer. Transition temperatures were determined by differential scanning calorimetry (Perkin–Elmer Diamond) with heating and cooling rates of 10 °C/min. The mesophases were studied by a polarizing optical microscope (Leica DMLP) equipped with a hot stage. Thermogravimetric analysis (TGA) was conducted on a Du Pont Thermal Analyst 2100 system with a TGA 2950 thermogravimetric analyzer under a heating rate of 20 °C/min. Gel permeation chromatography (GPC) analysis was conducted on a Water 1515 separation module using polystyrene as a standard and tetrahydrofuran (THF) as an eluant. UV-visible absorption spectra were recorded in dilute chloroform solutions (10^{-5} M) on a HP G1103A spectrophotometer, and fluorescence (PL and EL) spectra were obtained on a Hitachi F-4500 spectrophotometer. Polymer thin films were spin-coated on a quartz substrate from chloroform solutions with a concentration of 10 mg/ml (this condition consists with that of EL devices). Fluorescence quantum yields were determined by comparing the integrated PL density of a reference quinine sulfate in 0.1 M H_2SO_4 with a known quantum yield (ca. 1×10^{-5} M, quantum yield = 0.54) [26]. Cyclic voltammetry (CV) was performed at a scanning rate of 100 mV/s on a BAS 100 B/W electrochemical analyzer, which was equipped with a three-electrode cell. Pt wire was used as a counter electrode, and an Ag/AgCl was used as a reference electrode in the CV measurement. The polymer thin films were cast onto a Pt disc as a working electrode with ferrocene as a standard in acetonitrile, and 0.1 M tetrabutylammonium hexafluorophosphate ($TBAPF_6$) was used as a supporting electrolyte. A series of double-layer EL devices with the configuration of ITO/polymer/TPBI (30 nm)/MgAg (50 nm)/Ag (100 nm), in which 2,2′,2′-(1,3,5-phenylene)-tris[1-phenyl-1*H*-benzimidazole] (TPBI) as an electron transporting layer, were made by spin-coating the polymer solutions (with a concentration of 10 mg/ml in dichloroethane and the spin rate of 3000 rpm for 40 s) onto ITO glass substrates. The thickness of these films was measured on a Sloan DektakIIA surface profilometer, and the thicknesses of the polymer emitting layers were about 60 nm. The luminance-current-voltage characteristics were recorded on a power source (Keithley 2400) and photometer (MINOLTA CS-100A).

2.2. Materials

Chemicals and solvents were reagent grades and purchased from Aldrich, ARCROS, TCI, and Lancaster Chemical Co. Dichloromathane and THF were distilled to keep anhydrous before use. The other chemicals were used without further purification. The synthetic routes of monomers (**M1**–**M4**) are shown in Scheme 1.

2.2.1. 3,3′,5,5′-Tetrabromo-2,2′-bithiophene (1)

Bromine (14.58 g, 91.2 mmol) was added dropwise to a solution of 2,2′-bithiophene (7.12 g, 42.8 mmol) in a mixed solvent of glacial acetic acid (30 ml) and chloroform (77 ml) at a temperature of 5 °C. The mixture was stirred at room temperature for 5 h and then refluxed for 24 h. After the reaction was completed, the mixture was cooled to room temperature and 10% KOH aqueous was added. The mixture was extracted with chloroform and water, and the organic solvent was collected and removed by rotavapor. The residue was recrystallized from ethanol afforded yellow crystals in a yield of 85%. ^{1}H NMR ($CDCl_3$, 300 MHz, δ): 7.06 (s, 2H).

2.2.2. 3,3′-Dibromo-2,2′-bithiophene (2)

3,3′,5,5′-Tetrabromo-2,2′-bithiophene (9.81 g, 20.3 mmol) was added in portion to a zinc powder (5.33 g, 81.2 mmol) dispersion in 100 ml of ethanol containing 10 ml of water, 24 ml of acetic acid, and 2 ml of 2 M HCl aqueous. After refluxed for 2 h and then cooled to room temperature, the mixture was filtered and washed with ethanol, and filtrate was collected. After removed the solvent, the mixture was extracted with ether and water. The solvent was filtered and removed by rotavapor. Recrystallization from hexane afforded light yellow crystals in a yield of 71%. ^{1}H NMR ($CDCl_3$, 300 MHz, δ): 7.07 (d, J = 5.4 Hz, 2H), 7.40 (d, J = 5.4 Hz, 2H).

2.2.3. 3,3′-Diphenyl-2,2′-bithiophene (3)

A mixture of 3,3′-dibromo-2,2′-bithiophene (1.04 g, 3.2 mmol), benzeneboronic acid (1.20 g, 9.6 mmol), and tetrakis(triphenylphosphine) palladium (0.19 g, 0.16 mmol) were added in a degassed mixture of 1,2-dimethixyethane (DME) ([monomer] = 0.2 M) and aqueous 2 M sodium carbonate (3:2 in volume). The mixture was vigorously stirred at 85 °C for 48 h. After the mixture was cooled to room temperature, it was extracted with CH_2Cl_2 and water. The solvent was removed by rotavapor, the residue was purified by chromatograph (hexane). Yield: 86%. ^{1}H NMR

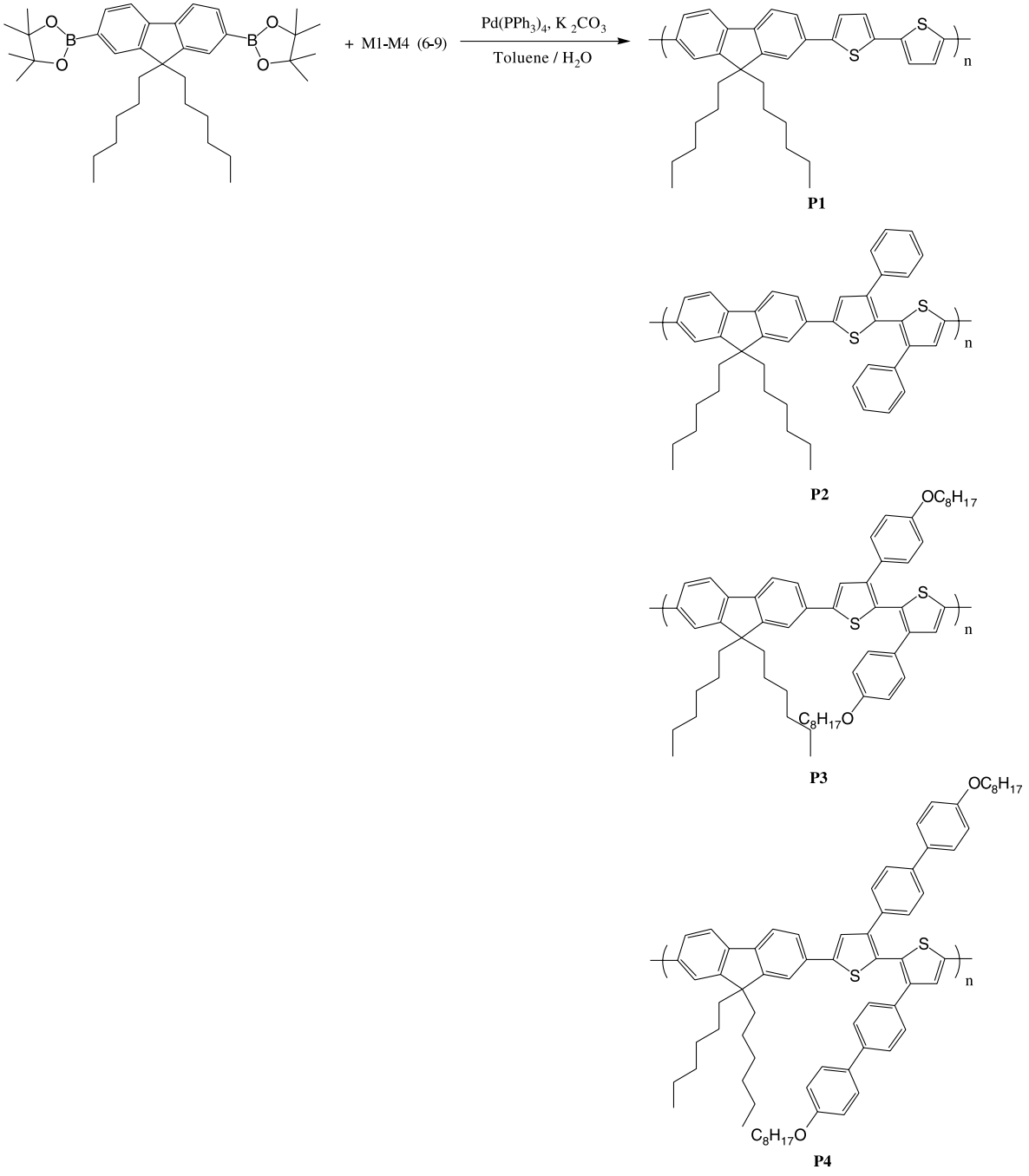

Scheme 2. Synthetic routes of polymers.

($CDCl_3$, 300 MHz, δ): 7.00–7.05 (m, 6H), 7.08–7.11 (m, 6H), 7.27 (d, $J=5.4$ Hz, 2H).

2.2.4. 3,3′-Bis-(4-octyloxy-phenyl)-2,2′-bithiophene (4)

3,3′-Bis-(4-octyloxy-phenyl)-2,2′-bithiophene was synthesized according to the procedure described for 3,3′-diphenyl-2,2′-bithiophene (3). Yield: 85%. ^{1}H NMR ($CDCl_3$, 300 MHz, δ): 0.88 (t, 6H), 1.28–1.43 (m, 20H), 1.72–1.76 (m, 4H), 3.88 (t, 4H), 6.66 (d, $J=8.4$ Hz, 4H), 7.00–7.05 (m, 6H), 7.25 (d, $J=5.4$ Hz, 2H).

2.2.5. 3,3′-Bis-(4′-octyloxy-biphenyl-4-yl)-2,2′-bithiophene (5)

3,3′-Bis-(4′-octyloxy-biphenyl-4-yl)-2,2′-bithiophenyl was synthesized according to the procedure described for 3,3′-diphenyl-2,2′-bithiophene (3). Yield: 78%. ^{1}H NMR ($CDCl_3$, 300 MHz, δ): 0.89 (t, 6H), 1.26–1.53 (m, 20H), 1.78–1.83 (m, 4H), 3.99 (t, 4H), 6.92 (d, $J=9$ Hz, 4H), 7.04 (d, $J=8.4$ Hz, 4H), 7.11 (d, $J=5.4$ Hz, 2H), 7.27 (d, $J=8.4$ Hz, 4H), 7.35 (d, $J=5.4$ Hz, 2H), 7.43 (d, $J=9$ Hz, 4H).

Table 1
Molecular weights and thermal properties of polymers **P1**–**P4**

Polymer	M_n	M_w/M_n	T_d[a] (°C)	T_g (°C)	T_m[b] (°C)
P1	41,800	1.90	442	129	>290
P2	9400	1.81	452	138	–
P3	14,400	1.61	436	120	–
P4	99,400	2.75	442	144	–

[a] Temperature of 5% weight loss measured by TGA in nitrogen.
[b] Melting temperature measured by polarizing optical microscopy (POM).

*2.2.6. **M2** (6). 5,5′-Dibromo-3,3′-diphenyl-2,2′-bithiophene*

N-Bromosuccinimide (0.98 g, 5.5 mmol) was added dropwise to a solution of 3,3′-diphenyl-2,2′-bithiophene (0.79 g, 2.5 mmol) in a mixed solvent of glacial acetic acid (3 ml) and chloroform (6 ml) at room temperature. The mixture was refluxed for 4 h. The mixture was extracted with CH_2Cl_2 and water, and the organic solvent was collected and removed by rotavapor. The residue was purified by chromatograph (CH_2Cl_2:hexane = 1:20). Yield: 94%. ^{1}H NMR ($CDCl_3$, 300 MHz, δ): 6.96–7.00 (m, 4H), 7.11–7.15 (m, 6H). Anal. Calcd for $C_{20}H_{12}Br_2S_2$: C, 50.44; H, 2.54. Found: C, 50.22; H, 2.90.

*2.2.7. **M3** (7). 5,5′-Dibromo-3,3′-bis-(4-octyloxy-phenyl)-2,2′-bithiophene*

5,5′-Dibromo-3,3′-bis-(4-octyloxy-phenyl)-2,2′-bithiophene was synthesized according to the procedure described for 5,5′-dibromo-3,3′-diphenyl-2,2′-bithiophene (6). Yield: 95%. ^{1}H NMR ($CDCl_3$, 300 MHz, δ): 0.90 (t, 6H), 1.26–1.44 (m, 20H), 1.74–1.78 (m, 4H), 3.90 (t, 4H), 6.69 (d, J = 8.4 Hz, 4H), 6.98–7.01 (m, 6H). Anal. Calcd for $C_{36}H_{44}Br_2O_2S_2$: C, 59.01; H, 6.05. Found: C, 58.79; H, 6.02.

*2.2.8. **M4** (8). 5,5′-Dibromo-3,3′-bis-(4′-octyloxy-biphenyl-4-yl)-2,2′-bithiophene*

5,5′-Dibromo-3,3′-bis-(4′-octyloxy-biphenyl-4-yl)-2,2′-bithiophene was synthesized according to the procedure described for 5,5′-dibromo-3,3′-diphenyl-2,2′-bithiophene (6). Yield: 95%. ^{1}H NMR ($CDCl_3$, 300 MHz, δ): 0.89 (t, 6H), 1.25–1.46 (m, 20H), 1.75–1.82 (m, 4H), 3.98 (t, 4H), 6.92 (d, J = 8.4 Hz, 4H), 7.00–7.04 (m, 6H), 7.28 (d, J = 8.4 Hz, 4H), 7.42 (d, J = 8.4 Hz, 4H). Anal. Calcd for $C_{48}H_{52}Br_2O_2S_2$: C, 65.15; H, 5.92. Found: C, 65.15; H, 5.93.

*2.2.9. **M1** (9). 5,5′-Dibromo-2,2′-bithiophene*

In the absence of light, *N*-bromosuccinimide (2.15 g, 11.9 mmol) was added dropwise to a solution of bithiophene (0.98 g, 5.8 mmol) in *N*,*N*-dimethylformamide (DMF) at room temperature. The mixture was stirred for 3 h at room temperature and poured into ice water, and the precipitate was filtered and washed with water and ethanol. Yield: 92%. ^{1}H NMR ($CDCl_3$, 300 MHz, δ): 6.84 (d, J = 3.9 Hz, 2H), 6.95 (d, J = 3.9 Hz, 2H). Anal. Calcd for $C_8H_4Br_2S_2$: C, 29.65; H, 1.24. Found: C, 29.81; H, 1.46.

2.3. Polymerization

The synthetic routes of polymers (**P1**–**P4**) are shown in Scheme 2. A general procedure of polymerization is proceeded through the Suzuki coupling reaction. A mixture of 2,7-bis-(4,4,5,5-tetramethyl-1,3,2-dioxaborolan-2-yl)-9,9-dihexyllfluorene (1 equiv), dibromo compound (1 equiv), and tetrakis(triphenylphosphine) palladium (1.0 mol%) were added in a degassed mixture of toluene ([monomer] = 0.2 M) and aqueous 2 M potassium carbonate (3:2 in volume). The mixture was vigorously stirred at 87 °C for 72 h. After the mixture was cooled to room temperature, it was poured into 200 ml of methanol. A fibrous solid was obtained by filtration. The solid was washed sequentially with methanol, water, and methanol.

P1. ^{1}H NMR ($CDCl_3$, 300 MHz, δ): 0.60–0.84 (m, 10H), 0.90–1.22 (m, 12H), 2.01 (br, 4H), 7.05–7.40 (m, 4H), 7.45–7.75 (m, 6H). Anal. Calcd for $C_{33}H_{36}S_2$: C, 79.79; H, 7.30. Found: C, 78.90; H, 6.98.

P2. Yield: 62%. ^{1}H NMR ($CDCl_3$, 300 MHz, δ): 0.71–0.92 (m, 10H), 1.09–1.20 (m, 12H), 2.04 (br, 4H), 7.05–7.21 (m, 10H), 7.38 (s, 2H), 7.59–7.72 (m, 6H). Anal. Calcd for $C_{45}H_{44}S_2$: C, 83.28; H, 6.83. Found: C, 80.01; H, 6.43.

P3. Yield: 70%. ^{1}H NMR ($CDCl_3$, 300 MHz, δ): 0.70–1.46 (m, 48H), 1.74–1.80 (m, 4H), 2.03 (br, 4H), 3.93 (t, 4H), 6.72 (d, J = 8.4 Hz, 4H), 7.12 (d, J = 8.4 Hz, 4H), 7.38 (s, 2H), 7.58–7.71 (m, 6H). Anal. Calcd for $C_{61}H_{76}O_2S_2$: C, 80.92; H, 8.46. Found: C, 80.34; H, 8.58.

P4. Yield: 83%. ^{1}H NMR ($CDCl_3$, 300 MHz, δ): 0.75–1.49 (m, 48H), 1.79–1.84 (m, 4H), 2.06 (br, 4H), 4.01 (t, 4H), 6.95 (d, J = 8.4 Hz, 4H), 7.15 (d, J = 8.1 Hz, 4H), 7.31 (d, J = 8.1 Hz, 4H), 7.42 (s, 2H), 7.46 (d, J = 8.4 Hz, 4H), 7.58–7.71 (m, 6H). Anal. Calcd for $C_{73}H_{84}O_2S_2$: C, 82.90; H, 8.01. Found: C, 83.12; H, 8.10.

3. Results and discussion

3.1. Synthesis and characterization

The synthetic routes of monomers (**M1**–**M4**) and polymers (**P1**–**P4**) are shown in Schemes 1 and 2. All these polymers were dissolved in common organic solvents to different degrees (**P1** < **P4** < **P2** < **P3**), and they form good transparent films on glass substrates. The number-average molecular weights (M_n) were measured by gel

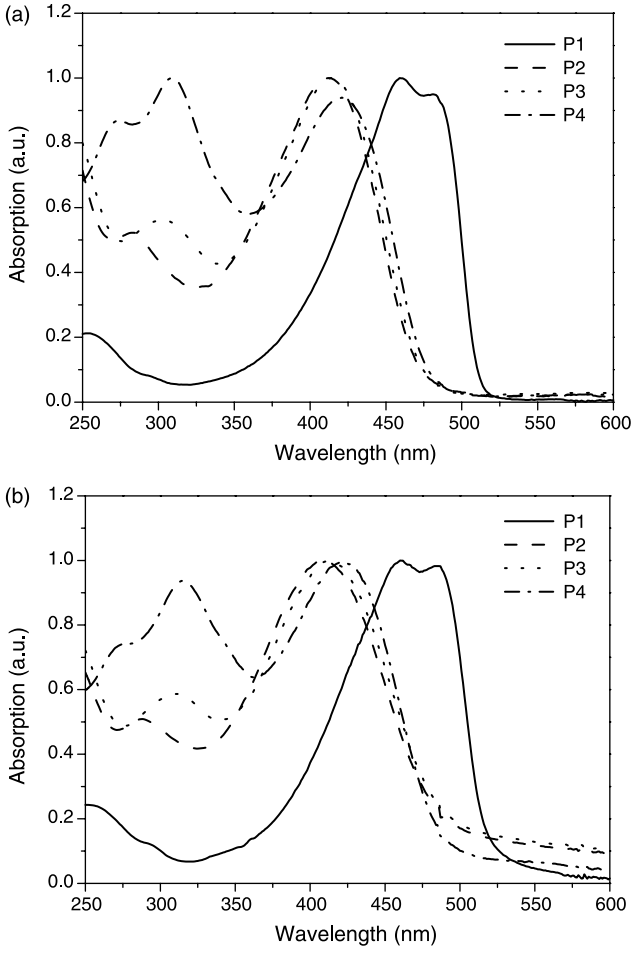

Fig. 1. UV–vis spectra of polymers (a) in dilute chloroform solutions (10^{-5} M). (b) In films.

permeation chromatography (GPC) with polystyrene as a standard and THF as an eluting solvent. The related data obtained from GPC are given in Table 1. The number-average molecular weights of the polymers were determined to be 9400–99,400 g/mol with polydispersity indexes of 1.61–2.75.

The thermal stability of the polymers (**P1**–**P4**) in nitrogen evaluated by thermogravimetric analysis (TGA) indicates that the degradation temperatures (T_d) of 5% weight loss in nitrogen are higher than 430 °C for all polymers (Table 1). The glass transition temperatures (T_g) and melting temperatures (T_m) of these polymers were determined by differential scanning calorimetry (DSC) in nitrogen atmosphere at a scanning rate of 10 °C/min and by polarizing optical microscopy (POM), correspondingly. Their glass transition temperatures are shown between 120 and 144 °C, which are higher than poly(9,9-dihexylfluorene) (~75–80 °C) [27] and also higher than most other fluorene-based copolymers [28]. Comparing **P4** with **P1**, when biphenyl groups are attached to 3,3′-position of bithiophene, an increase of 15 °C in T_g is observed in **P4**. That may originate from the contribution of the rigidity of the biphenyl side groups (due to the steric hindrance of the bulky biphenyl side groups) and/or the higher molecular weight of **P4**. Besides, **P1** exhibits mesomorphism at high temperatures (>290 °C), but **P2**–**P4** do not exhibit any mesophase. This may be because that bulky side substituents of bithiophene interrupt the interactions between rigid cores and prohibit from liquid crystalline packing. Another reason is that maybe the diaryl substituents disperse the dipole moments of the main chains in polymers to reduce the mesogenic interactions. With diaryl substituents on bithiophene units, the relatively high glass transition temperatures of molecular architectures are necessary for PLED applications as an emission layer, and the thermal stabilities will improve operating lifetime of PLED devices.

3.2. Optical properties

The UV–visible absorption spectra of these polymers are shown in Fig. 1. The larger λ_{max} values in the region of 370–500 nm are attributed to the electron transition of π–π* along the conjugated backbones of the polymers. It is noticed that **P1** exhibits a much larger absorption λ_{max} value than **P2**–**P4**. The blue shift of the absorption maxima in **P2**–**P4** may be ascribed to loss coplanarity of backbones in the polymers. The bulky substituents on 3,3′-positions of thiophene rings give steric hindrance between the side groups and/or the adjacent thiophene rings thus to result in the distortion of the backbones in **P2**–**P4**. Therefore, the conjugation of polymer backbones is interrupted which induces a blue shift of the absorption maximum. Comparing **P2** with **P3**, two polymers show almost identical absorption spectra. It is obvious that the alkoxy side chains on the pendants of the thiophene do not have any noticeable influence on the absorption spectra of polymers.

The shorter wavelengths (in the range of 270–350 nm) of absorption spectra may originate from the absorption of the

Table 2
PL emission spectral data of polymers in chloroform solutions and thin solid films

Polymer	$\lambda_{PL,sol}$ (nm)	$\lambda_{PL,film}$ (nm)	$FWHM_{sol}$ (nm)	$FWHM_{film}$ (nm)	$\Phi_{PL,sol}$[a]	Rel. $\Phi_{PL,film}$[a]
P1	506 (537)[b]	543 (514)[b]	55	87	0.42	1
P2	507	514	78	81	0.05	0.33
P3	509	514	76	78	0.04	0.41
P4	515	517	83	84	0.04	0.69

[a] Excited at the absorption region of polymer backbones.
[b] Data in parentheses are the second major peaks.

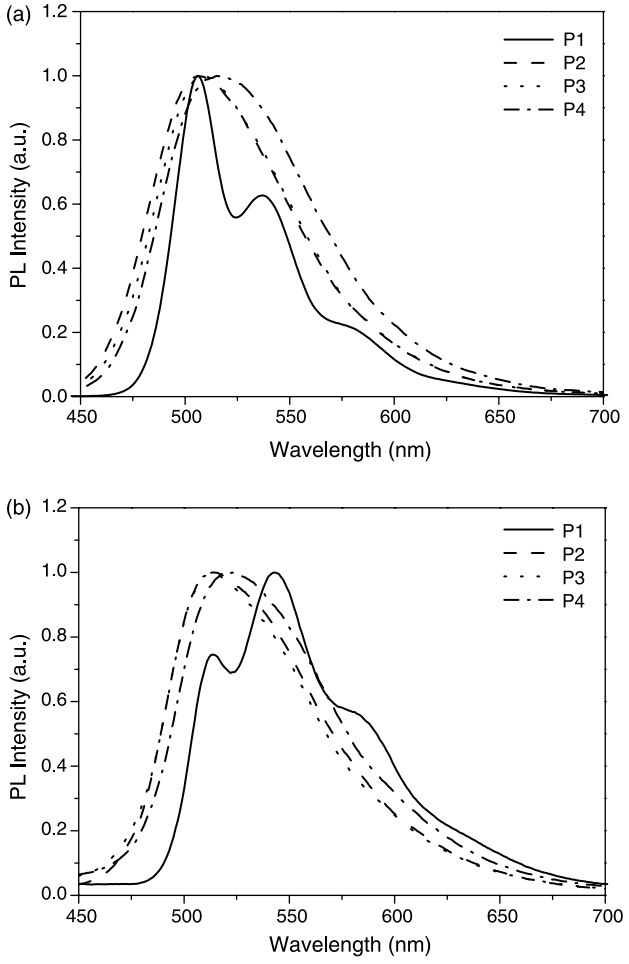

Fig. 2. Spectra of polymers (a) in dilute chloroform solutions (10^{-5} M). (b) In films.

substituents, and the intensities of absorption increase with longer conjugation lengths of the substituents. Comparing UV-visible spectra of thin films with diluted solutions, although the polymer main-chain absorption peaks of the solution and film samples are similar, all polymers show tails in the low energy regions. This result indicates some extents of ground-state aggregation exist in the solid state, especially in **P1**. Therefore, it is obvious that the pendant groups of bithiophene units have strong influence on the absorption of polymers.

The optical band gap energies obtained from UV-visible absorption spectra in solutions are also given in Table 3. The band gap energies of polymers were determined by the intersection of the tangent through the turning point of the lower energy side of the spectrum and the lengthened baseline for each polymer. The optical band gap of **P1** is measured to be 2.43 eV. Nevertheless, diaryl-substituted polymers (**P2–P4**) have blue-shifted absorption curves and larger band gaps (2.61–2.63 eV). It is because that the head-to-head configurations of 3,3′-disubtituted bithiophene units in these polymers lead to an increase of repulsive interactions between the thiophene rings themselves and/or between thiophene and adjacent fluorene rings, which force the backbones out of coplanarity. Therefore, **P2–P4** have larger band gaps due to the shorter conjugation lengths by the twisting of the backbones which is induced by the side diaryl-substituted groups. Nevertheless, the optical band gaps of **P2–P4** are almost indistinguishable, regardless of the differences in polarities and rigidities of phenyl and biphenyl rings among the substituents.

The PL quantum yield (Φ_{PL}), PL emission maxima (λ_{PL}), and full width at half-maximum (FWHM) values of these polymers are exhibited in Table 2. All emission data were obtained by the excitation at the absorption regions of polymer backbones. The PL emission spectra in dilute solutions as well as in thin films are shown in Fig. 2, where these polymers exhibit green emissions from the polymer backbones. **P2–P4** only show one PL emission peak ranging from 507 to 515 nm in dilute solutions, and they show red shifts of PL emissions ca. 2–7 nm in thin films. On the contrary, **P1** shows two well-resolved excimer bands in both of the solution and solid states, and due to strong aggregation it even forms a dominant PL excimer peak (~543 nm) in the solid state. This phenomenon suggests that the bulky substitutents at 3,3′-positions of bithiophenes can efficiently reduce aggregation in the solid state and enhance the amorphism of the polymers. Comparing absorption and PL spectra of **P1** with those of **P2–P4** in solutions, the absorption maxima of **P2–P4** are blue-shifted ca. 38–47 nm, but PL emission maxima of **P2–P4** are slightly red-shifted ca. 1–9 nm. This result indicates **P2–P4** have shorter conjugated lengths than **P1** in the ground state, but **P2–P4** have longer conjugated lengths similar to **P1** in the excited state. As for diaryl-substituted polymers (**P2–P4**), compared with the PL spectra in solutions, the PL emission peaks in solid films only show small red shifts (the maximum red-shifted value is 7 nm). However, in contrast to diaryl-substituted polymers, the PL peak of **P1** in thin

Table 3
HOMO and LUMO energies, and electrochemical properties of polymers **P1–P4**

Polymer	$E^{ox/onset}$ (V)	$E^{ox/peak}$ (V)	E^{HOMO} (eV)	E^{LUMO} (eV)[a]	Optical band gap (eV)
P1	0.72	0.76, 1.24	−5.07	−2.64	2.43
P2	0.84	0.91, 1.20	−5.19	−2.56	2.63
P3	0.79	0.87, 1.07	−5.14	−2.51	2.63
P4	0.77	0.89, 1.38	−5.12	−2.51	2.61

[a] LUMO values of polymers are obtained by deduction of optical band gap values from HOMO values due to the lack of reduction peaks in CV measurements.

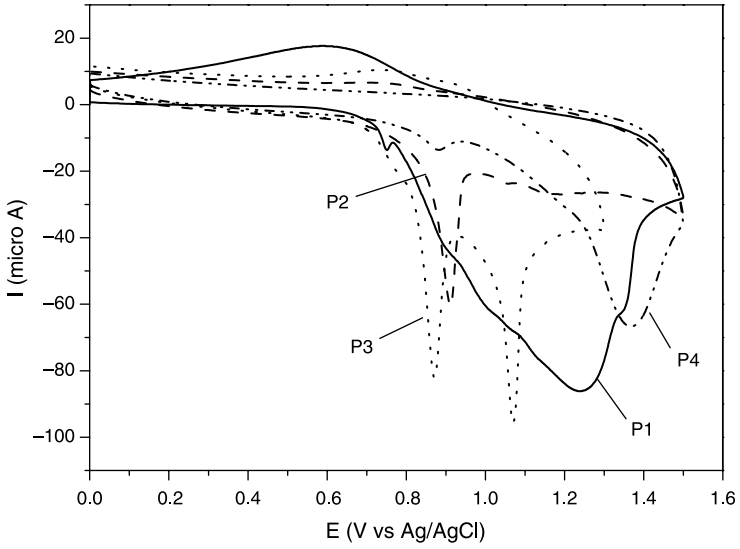

Fig. 3. Cyclic voltammetry of polymers during the oxidation process.

films is red-shifted 37 nm (from 506 nm in solutions to 543 nm in films) and the emission peak of 543 nm becomes a dominated emission peak, which is due to the aggregation of polymer chains in the solid state of non-substituted **P1**.

It is interesting to note that the PL quantum yields of diaryl-substituted polymers (**P2**–**P4**) are much lower than that of non-substituted polymer (**P1**) in Table 2. This phenomenon is similar to our previous report and other literatures [29–32]. The PL quantum yields will be decreased when the pendant groups (side chains) are conjugated with the polymer main chains. It may be due to the multifarious conjugated forms in the conjugated substituents of bithiophene units, which cannot confine the excitons efficiently; hence, the PL quantum yields drop considerably in the diaryl-substituted polymers. On the other hand, the PL quantum yields of **P2**–**P4** in solutions are quite similar, indicating that the variation of side-chain diaryl substituents on bithiophene units have little effect on PL quantum yields of the polymers based on the same structures of polymer backbones. However, the quantum yields in films increase in the order of **P2**<**P3**<**P4** according to the size of pendant groups (Table 2). This result can be explained by the large steric hindrance of the pendant groups to restrain diaryl-substituted polymers from interchain interactions in solids, so the quantum yields of diaryl-substituted polymers with larger pendant groups are enhanced. The effect of large steric hindrance can also be observed when comparing emission peaks and FWHM in solution and solid states, respectively (Table 2). Comparing λ_{PL} and FWHM values of solution and solid states, **P4** has the least red shift of 2 nm (from 515 nm in solutions to 517 nm in films) in the PL emission peak (λ_{PL}) and the smallest change of 1 nm (from 83 nm in solutions to 84 nm in films) in the value of FWHM of the emission peak.

3.3. Electrochemical properties

Cyclic voltammetry (CV) is used to estimate the band gaps, electron affinities, and work functions of conjugated polymers. The potentials were based on the reference energy level of ferrocene (4.8 eV below the vacuum level) according to the following equation [26]: $E^{HOMO}/E^{LUMO} = [-(E^{onset}-0.45)-4.8]$ eV. The onset potentials were determined from the intersection of two tangents drawn at the rising and background currents of the cyclic voltammogram. Since the onset of the oxidation potentials (i.e. $E^{ox/onset}$) for the polymers were obtained from the cyclic voltammetry measurements, the HOMO (i.e. E^{HOMO}) values were calculated from the previous equation, i.e. $E^{HOMO} = [-(E^{ox/onset}-0.45)-4.8]$ eV. The reduction potential peaks of the polymers were not observed in the CV measurements, so crude estimations of LUMO values in reduction processes of polymers are made by deduction of optical band gap values from HOMO values. HOMO and LUMO energies, and electrochemical properties (from CV measurements) of polymers (**P1**–**P4**) are shown in Table 3.

Table 4
PLED device performance data

Polymer	λ_{max} (nm)	V_{on}[a] (V)	Max. brightness (cd/m^2) (V)	FWHM$_{EL}$ (nm)
P1[b]	520	4.0	12 (11.0)	90
P2[b]	516	4.0	1265 (13.5)	84
P3[b]	515	3.5	2590 (9.5)	78
P4[b]	528	2.4	474 (11.5)	92
P3[c]	518	3.5	4284 (18)	82

[a] V_{on} is the turn-on voltage of light.
[b] Device structure: ITO/polymer/TPBI (30 nm)/MgAg (50 nm)/Ag (100 nm).
[c] Device structure: ITO/PVK:**P3** (100:30 by weight) (60 nm)/TPBI (30 nm)/MgAg (50 nm)/Ag (100 nm).

Table 5
PLED device performance data measured at 100 mA/cm^2

Polymer	Voltage (V)	Brightness (cd/m^2)	Luminance efficiency (lm/W)	Power efficiency (cd/A)	External Q.E. (%)
P1[a]	5.4	2	0[c]	0[c]	0[c]
P2[a]	5.5	110	0.06	0.11	0.04
P3[a]	6.7	932	0.44	0.94	0.29
P4[a]	6.5	40	0.02	0.04	0.01
P3[b]	7.5	1025	0.43	1.03	0.46

[a] Device structure: ITO/polymers/TPBI (30 nm)/MgAg (50 nm)/Ag (100 nm).
[b] Device structure: ITO/PVK:**P3** (100:30 by weight) (60 nm)/TPBI (30 nm)/MgAg (50 nm)/Ag (100 nm).
[c] Too small to be detected.

These polymers have the same backbone structures of poly(fluorene-*co*-*alt*-bithiophene) with different substituents on 3,3′-position of bithiophene units. It is interesting to evaluate that how these pendants modulate the electrochemical behavior of these polymers. As shown in Fig. 3, the polymers possess two anodic peaks at potentials ranging from 0.76 to 1.38 V (Table 3) and onset potentials of oxidation between 0.72 and 0.84 V in anodic scans. Compared with **P1**, it seems that the onset potentials of oxidation of **P2**–**P4** slightly larger than **P1**. This result reveals that **P1** has a smaller band gap than **P2**–**P4**. Compared with **P2**, the oxidized onset potentials of **P4** are not remarkably changed by the replacement of phenyl groups with π-extended biphenyl groups.

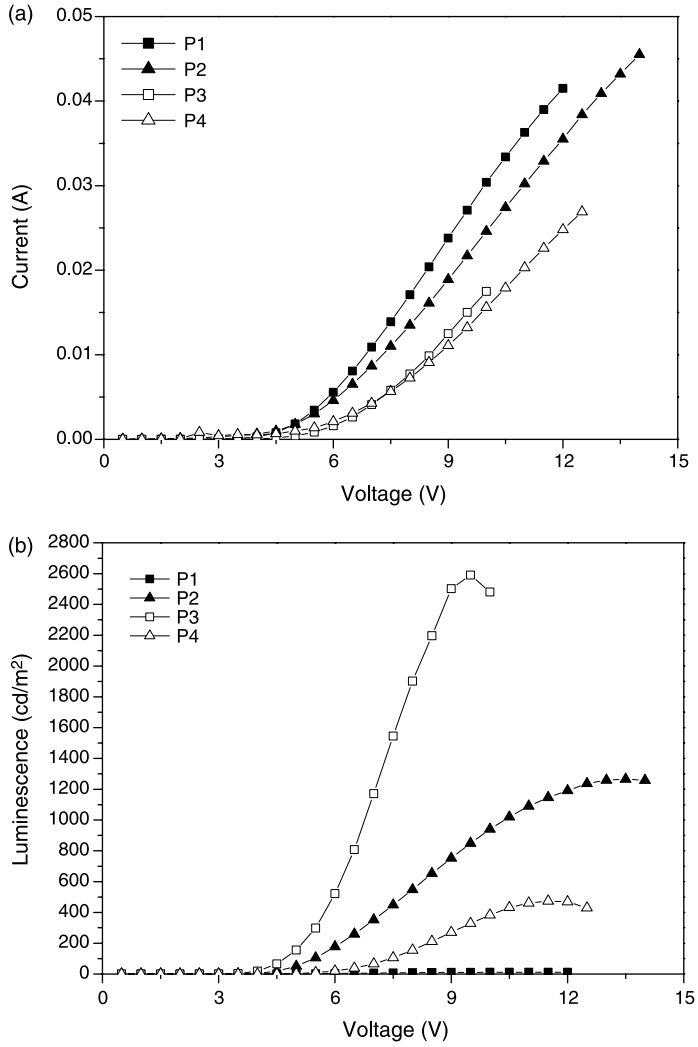

Fig. 4. (a) Current-voltage and (b) luminescence-voltage characteristics of ITO/polymer/TPBI (30 nm)/MgAg (50 nm)/Ag (100 nm) devices.

3.4. Electroluminescent (EL) properties of PLED devices

The PLED device performance data are summarized in Tables 4 and 5. The current-voltage and luminescence-voltage characteristics are displayed in Fig. 4. These devices show turn on voltages for light at ca. 2.4–4 V, and the device of **P4** with device structure: ITO/polymer/TPBI (30 nm)/MgAg (50 nm)/Ag (100 nm) has the lowest turn-on voltage (2.4 V). Though the non-substituted polymer (**P1**) has the highest PL quantum yield in solutions (in chloroform), the PLED device of **P1** has the worst emission properties due to the poor solubility of **P1** in dichloroethane during the spin-coating process. Hence, the device luminance order (**P1** < **P4** < **P2** < **P3**) is approximately followed by the solubility order of the polymers in dichloroethane. Due to the highest solubility of **P3** in dichloroethane, the device with **P3** as an emitter has the highest luminance of 2590 cd/m^2 at 9.5 V (with a power efficiency of 0.94 cd/A and an external quantum yield of 0.29% at 100 mA/cm^2) among these polymers (Tables 4 and 5), and shows stable emission with increasing operating voltages. The device performance can be further improved by blending polymers with poly(*N*-vinyl carbazole) (PVK), i.e. PVK:**P3** = 100:30 by weight in device structure: ITO/PVK:**P3** (100:30 by weight) (60 nm)/TPBI (30 nm)/MgAg (50 nm)/Ag (100 nm), a bright luminance of 4284 cd/m^2 at 18 V (with a power efficiency of 1.03 cd/A and an external quantum yield of 0.46% at 100 mA/cm^2) can be reached (Tables 4 and 5). The device performance is probably improved by the film uniformity of PVK or by electron blocking of the interface between PVK and TPBI.

Most EL spectra are well matched with the corresponding PL emission spectra of thin films, which indicates that comparable fluorescent emissions of excited states are involved in both EL and PL processes. As shown in Fig. 5(a), EL emission spectra of these polymers are alike at 8 V, and exhibit similar EL and PL spectra in solid films, except **P1**. Moreover, emission peaks around 380 nm attributed to TPBI emission were perceptible in PLED devices with the device configuration: ITO/polymer/TPBI (30 nm)/MgAg (50 nm)/Ag (100 nm). The TPBI emission peaks were observed to different degrees, in the order of **P1** > **P4** > **P2** > **P3**, depending on the emission intensities of the major emission in the polymers. Compared with PL spectra of **P1**, a dominant PL excimer peak (~543 nm) in the solid state may be suppressed or shifted to 520 nm in EL spectra due to a stronger emission from TPBI. Fig. 5(b) shows that the EL spectra of **P3** are almost unchanged and without any TPBI emission bands (due to the bright major emission of **P3**) as the voltage increases from 6 to 10 V. Thus, this PLED device demonstrates good EL properties without voltage dependent effects. Fig. 6 shows EL spectra of **P3** blended with PVK in the ratio of PVK:**P3** = 100:30 by weight, as can be seen that the intensity of 380 nm TPBI emission peak ca. 380 nm will increase as the voltage increases. This result implies that PVK can block electrons in the interface between PVK and TPBI, which results in growing emission intensities of TPBI by increasing voltages.

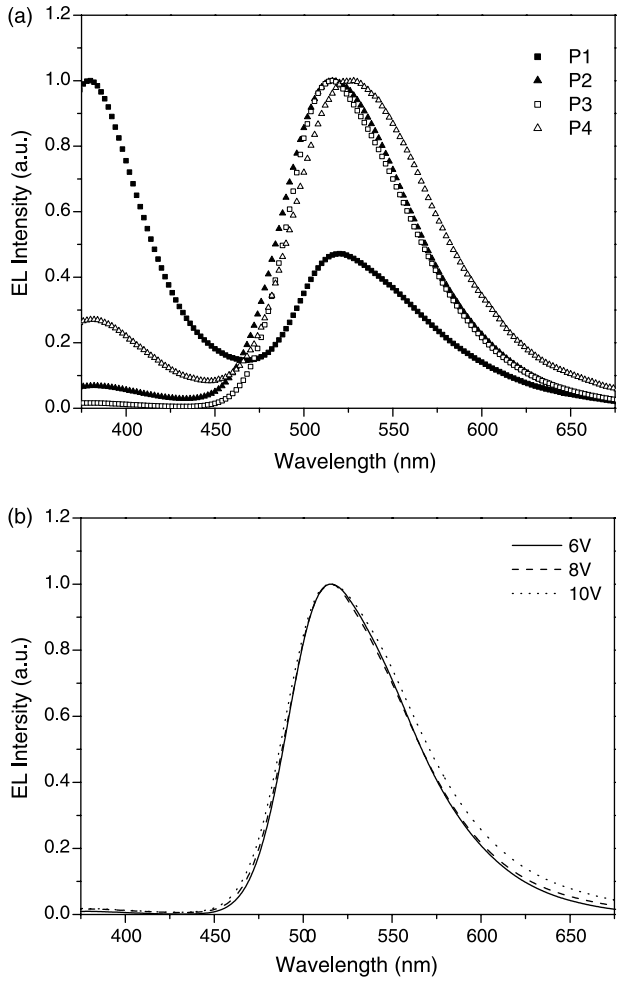

Fig. 5. (a) Normalized EL spectra of ITO/polymer/TPBI (30 nm)/MgAg (50 nm)/Ag (100 nm) devices operating at 8 V. (b) Normalized EL spectra of ITO/P3/TPBI (30 nm)/MgAg (50 nm)/Ag (100 nm) device operating at different voltages.

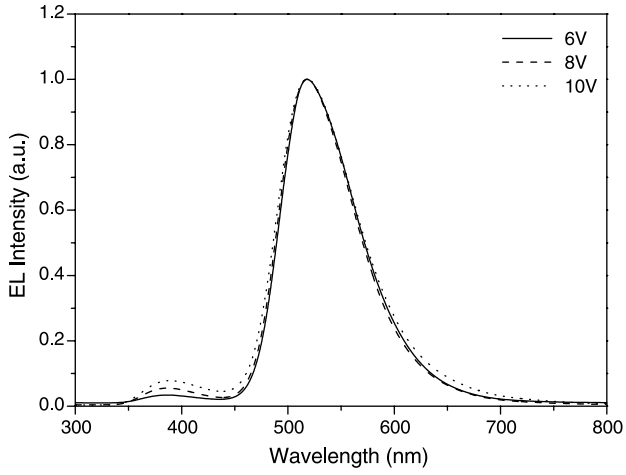

Fig. 6. Normalized EL spectra of ITO/PVK:P3 (100:30 by weight)/TPBI (30 nm)/MgAg (50 nm)/Ag (100 nm) device operating at different voltages.

4. Conclusions

- These polymeric bithiophene derivatives incorporating with fluorenes exhibit relatively high T_g and good thermal stabilities.
- Owing to the large steric hindrance of diaryl substituents on bithiophenes, the aggregation of the polymers (**P2–P4**) in solids is reduced. Therefore, even though the PL quantum yields of diaryl-substituted polymers (**P2–P4**) are much lower than that of non-substituted polymer (**P1**), the performance of their PLED devices are superior to that of **P1**.
- Compared with the non-substituted polymer (**P1**), the introduction of diaryl substitutents at 3,3′-positions of bithiophene units in **P2–P4** has significant effects on the photophysic properties of resulting polymers in solution and solid states. However, different diaryl substituents on bihiophene units only affect the electronic properties of the resulting polymers slightly.
- Consequently, the device made of **P3** as an emitter has the highest luminance of 2590 cd/m^2 at 9.5 V among these polymers. For optimum device performance, a device of **P3** blended with PVK can be further enhanced to a brighter luminance of 4284 cd/m^2 at 18 V.

Acknowledgements

We are grateful for the financial support provided by the National Science Council of Taiwan, ROC through NSC 92-2113-M-009-016.

References

[1] Redecker M, Bradley DDC, Inbasekaran M, Woo EP. Appl Phys Lett 1998;73:1565.
[2] Grell M, Bradley DDC, Ungar G, Hill J, Whitehead KS. Macromolecules 1999;32:5810.
[3] Klaerner G, Miller RD. Macromolecules 1998;31:2007.
[4] Chen X, Liao JL, Liang Y, Ahmed MO, Tseng HE, Chen SA. J Am Chem Soc 2003;125:636.
[5] Jenekhe SA, Osaheni JA. Science 1994;265:765.
[6] Weinfurthner KH, Fujikawa H, Tokito S, Taga Y. Appl Phys Lett 2000;76:2502.
[7] Pei Q, Yang Y. J Am Chem Soc 1996;118:7416.
[8] Kim JS, Friend RH, Cacialli F. Appl Phys Lett 1999;74:3084.
[9] Ego C, Grimsdale AC, Uckert F, Yu G, Srdanov G, Mullen K. Adv Mater 2002;14:809.
[10] Wu FI, Reddy S, Shu CF, Liu MS, Jen AKY. Chem Mater 2003;15:269.
[11] Shu CF, Dodda R, Wu FI, Liu MS, Jen AKY. Macromolecules 2003;36:6698.
[12] Sung HH, Lin HC. J Polym Sci, Part A: Polym Chem 2005;43:2700.
[13] Andersson MR, Berggren M, Inganas O, Gustafsson G, Gustafsson-Carlberg JC, Selse D, et al. Macromolecules 1995;28:7525.
[14] Kham K, Sadki S, Chevrot C. Synth Met 2004;145:135.
[15] Naudin E, Mehdi NE, Soucy C, Breau L, Belanger D. Chem Mater 2001;13:634.
[16] Xu B, Holdcroft S. Macromolecules 1993;26:4457.
[17] Albert IDL, Marks TJ, Ratner MA. J Am Chem Soc 1997;119:6575.
[18] Janietz S, Bradley DDC, Grell M, Giebeler C, Inbasekaran M, Woo EP. Appl Phys Lett 1998;73:2453.
[19] Ruiz JP, Dharia JR, Reynolds JR, Buckley LJ. Macromolecules 1992;25:849.
[20] Chen ZK, Meng H, Lai YH, Huang W. Macromolecules 1999;32:4351.
[21] Meng H, Yu WL, Hunang W. Macromolecules 1999;32:8841.
[22] Pu YJ, Soma M, Kido J, Nishide H. Chem Mater 2001;13:3817.
[23] Aleman C, Julia L. J Phys Lett 1996;100:14661.
[24] (a) Demadrille R, Divisia-Blohorn B, Zagorska M, Quillard S, Rannou P, Traversa JP, et al. New J Chem 2003;27:1479.
(b) Demadrille R, Patrice R, Bleuse J, Oddou JL, Pron A, Zagorska M. Macromolecules 2003;36:7045.
[25] (a) Lim E, Jung BJ, Shim HK. Macromolecules 2003;36:4288.
(b) Liu B, Yu WL, Lai YH, Huang W. Macromolecules 2000;33:8945.
[26] Egbe DAM, Cornelia B, Nowotny J, Gunther W, Klemm E. Macromolecules 2003;36:5459.
[27] (a) Zeng G, Yu WL, Chua SJ, Huang W. Macromolecules 2002;35:6907.
(b) Marsitzky D, Murray J, Scott JC, Carter KR. Chem Mater 2001;13:4285.
[28] (a) Chen Y, Araki Y, Doyle J, Strevens A, Ito O, Blau WJ. Chem Mater 2005;17:1661.
(b) Kreyenschmidt M, Klaerner G, Fuhrer T, Ashenhurst J, Karg S, Chen WD, et al. Macromolecules 1998;31:1099.
[29] Sung HH, Lin HC. Macromolecules 2004;37:7945.
[30] Lee YZ, Chen X, Chen SA, Wei PK, Fann WS. J Am Chem Soc 2001;123:2296.
[31] Xu B, Pan Y, Zhang J, Peng Z. Synth Met 2000;114:337.
[32] (a) Liu MS, Jiang X, Herguth P, Jen AKY. Chem Mater 2001;13:3820.
(b) Wilson JN, Windscheif PM, Evans U, Myrick ML, Bunz UHF. Macromolecules 2002;35:8681.